



## Direct molecular level characterization of different heterogeneous freezing modes on mica

Ahmed Abdelmonem<sup>1</sup>

<sup>1</sup>Institute of Meteorology and Climate Research – Atmospheric Aerosol Research (IMKAAF), Karlsruhe Institute of Technology (KIT), 76344 Eggenstein-Leopoldshafen, Germany

*Correspondence to:* Ahmed Abdelmonem (ahmed.abdelmonem@kit.edu)

**Abstract.** The mechanisms behind heterogeneous ice nucleation are of fundamental importance to the prediction of the occurrence and properties of many cloud types, which influence climate and precipitation. Aerosol particles act as cloud condensation and freezing nuclei. The surface–water interaction of an ice nucleation particle plays a major, not well explored, role in its ice nucleation ability. This paper presents a real–time–molecular–level comparison of different freezing modes on the surface of an atmospherically relevant metal oxide surface (mica) under varying supersaturation conditions using second harmonic generation spectroscopy. Two sub-deposition nucleation modes were identified (one- and two-stage freezing). The nonlinear signal at water–mica interface was found to drop upon the formation of a thin film on the surface regardless of 1) the formed phase (liquid or ice) and 2) the freezing path (one– or two–step), indicating similar molecular structuring. The results also revealed a transient phase of ice at water–mica interfaces during freezing, which has a lifetime of around one minute. Such information will have a significant impact on climate change, weather modification, and tracing of water in hydrosphere studies.

### 1 Introduction

Clouds influence the energy budget by scattering sunlight and absorbing heat radiation from the earth and are therefore considered the major player in the climate system. Formation of ice changes cloud dynamics and microphysics because of the release of latent heat and the Bergeron-Findeisen process, respectively (Pruppacher and Klett, 1997). Ice nucleation in the atmosphere can be triggered heterogeneously by aerosol particles, ice-nucleating particles (INP), or occurs homogeneously at about -38°C (Pruppacher and Klett, 1997). Cloud evolution depends not only on temperature and humidity, but also on the abundance and surface characteristics of atmospheric aerosols. Understanding the factors that influence ice formation within clouds is a major unsolved and pressing problem in our understanding of climate (Slater et al., 2016). Field and laboratory experiments on cloud formation started decades ago (see (Schaefer, 1949; DeMott et al., 2011; Hoose and Mohler, 2012) and references therein) and are ongoing. A wide variety of results and observations has been obtained in cloud microphysics, especially with respect to the ice nucleation ability of atmospheric aerosol particles and, hence, the mechanisms of cloud dynamics, precipitation formation, and interaction with incoming and outgoing radiation. Aerosol particles act as cloud condensation nuclei for liquid clouds, immersion or contact freezing nuclei for mixed-phase clouds, and heterogeneous deposition nuclei for ice (cirrus) clouds. Depending on whether water nucleates ice from the vapor or the supercooled liquid phase, ice nucleation is classified as deposition nucleation or immersion nucleation, respectively. Despite numerous investigations aimed at characterizing the effect of particle size and surface properties of the INP, there is a lack of information about the restructuring of water molecules on the surface of INPs around the heterogeneous freezing point.

In this paper, discrimination between different modes of freezing of water on an ice-nucleating surface using nonlinear optical spectroscopy is demonstrated. Mica, a widely spread layered clay mineral and one of the most prominent mineral



surfaces due to its atomic flatness and chemical inertness produced by perfect cleavage parallel to the 001 planes (Poppa and Elliot, 1971), was selected as a model surface in this study. Mica, as natural particles, is believed to be among the most effective ice nucleating minerals in the deposition mode (Eastwood et al., 2008; Mason and Maybank, 1958). An early study of deposition nucleation of ice on freshly cleaved mica using a projection microscope, revealed that there is no growth of ice until saturation with respect to water is reached (Layton and Jr., 1963). The authors concluded that at temperatures above -40 °C, the growth of ice on mica should be a two-step process: A nucleus forms as water and then freezes. Experimental evidence of two-step nucleation was also provided by (Campbell et al., 2013) using an optical microscope. With the help of a scanning optical microscope, they showed that nucleation favored specific nucleation sites. However, they suggested that a supercooled liquid phase forms first and then freezes after it has grown to a size which thermodynamically favors the solid phase. These assumptions were based merely on thermodynamic observations (temperature and vapor supersaturation). Recent MD simulations of deposition freezing revealed that water first deposits in the form of liquid clusters and then crystallizes isothermally from there (Lupi et al., 2014). So far, there has been no direct experimental evidence of two-step freezing based on probing the molecular structuring of water molecules next to the surface.

In this work, second-harmonic generation (SHG) in total internal reflection (TIR) geometry was used to probe the change in the degree of ordering of water on the surface of mica. SHG is a powerful and simple, compared to sum-frequency generation (SFG), surface-sensitive spectroscopic tool for studying molecules near surfaces and at interfaces (Shen, 1989a; Shen, 1989b). The amplitude and polarization of the generated field, as a function of the polarization of the incident fields, carry information on the abundance and structure of the interfacial molecules between two isotropic media (Jang et al., 2013; Rao et al., 2003; Zhuang et al., 1999). In the system described here, the SHG signal is originated from the nonresonant OH stretching vibrations at the interface. The signal response relates to the overall arrangements of the interfacial entities (Fordyce et al., 2001; Goh et al., 1988; Luca et al., 1995). More details of SHG and SFG can be found in SI. The results provide new insight into heterogeneous freezing processes and show the suitability of the method for studying current issues relating to ice nucleation, which will contribute to its rapid development in the next years. Initially, I found that the SHG signal drops upon the formation of a thin film regardless of whether the freezing path consists of one- or two-steps and the initially formed phase, liquid or ice, indicating a similar molecular structuring. In addition, I observed a transient SHG signal after immersion freezing.

The hygroscopicity of mica is expected to play a role in the described processes. The hygroscopicity and Langmuir isotherm studies on mica are available in literature but only at room temperature where the sample and environment are at equilibrium (Balmer et al., 2008; Beaglehole et al., 1991; Hu et al., 1995). Such studies at supercooled surfaces are worth to do and could be a topic of future work. An AFM study at 21 °C showed no water absorbed on the surface of mica at RH = 18 % (Hu et al., 1995). The first uniform water phase, of large two-dimensional islands with geometrical shapes in epitaxial relation with the underlying mica lattice, was observed at RH = 28 %. The growth of this water phase is completed when the humidity reaches 40 to RH = 50 %. In my experiments on mica it is not possible to detect sub-monolayers, at least at this stage, due to technical reasons mentioned later. In the presented work, only clear steps in the signal were considered.

## 2 Experimental

### 2.1 Materials and setup

All experiments were carried out using MilliQ water (18.2 MΩ·cm). The total organic content in this water is below 4 ppb. Mica samples were obtained from Plano GmbH, Germany. The mica samples were freshly cleaved parallel to the 001 plane in air right before use. The freshly cleaved mica exhibits a wetting surface (on which water was spreading visually). The supercooled SHG setup and the measuring cell were described in previous publications (Abdelmonem et al., 2015; Abdelmonem et al., 2017). Briefly, in the SHG experiments a sapphire prism is used as an optical coupler to the



surface of a thin mica substrate, the basal plane of which is exposed to liquid water or water vapor. To study mica in TIR geometry, an index matching gel (IMG) is used to fix the mica sample on the hypotenuse of the sapphire prism. A detailed description of sample geometry and the selection of the IMG was published in (Abdelmonem et al., 2015). A temperature-controlled environmental chamber was integrated into the setup to control the sample temperature. A commercially available  
5 cold stage (Linkam model HFS-X350) was used after modifying the housing to accommodate the SHG setup. Control software was developed to adhere to a predefined temperature profile and to measure the SHG signal and the temperature of the substrate. Temperature profiles were repeated several times for each sample to test reproducibility. In each run, the sample was heated to 110 °C while purging with N<sub>2</sub> gas (99.9999 %) to evaporate any residual water, then cooled down to 0 °C at a rate of 10 °C/min and then down to the heterogeneous freezing point at a rate of 1 °C/min. This cooling profile was  
10 the same for all runs to allow for logical comparison.

An experiment with a mica-N<sub>2</sub> gas interface was carried out to ensure that the change in the refractive indices of the sapphire prism, IMG, and mica substrate had no significant effect on the resulting SHG signal in the range of temperatures applied in this work. During the freezing experiments, the substrate of interest was sealed to a circular opening of 8 mm in diameter in a teflon cell which was purged with a dry-humid air mixture. The prism was inserted into a tight housing of the  
15 cooling/heating stage. The temperatures of the sample top, sample bottom, and air mixture inside the cell were recorded using four-wire-Pt100 elements. This was not done to determine the exact onset conditions of freezing, but rather to study the qualitative behavior of water molecules during freezing on the different paths. The humidity of the gas mixture pumped to the measuring cell was adjusted by mixing N<sub>2</sub> gas with saturated water vapor at room temperature (21 °C). The mixing ratio was set using Tylan 2900 flow controllers.

20 The SHG experiments were conducted using a femtosecond laser system (Solstice, Spectra Physics) with a fundamental beam of 800 nm wavelength, 3.5 mJ pulse energy, ~80 fs pulse width, 1 kHz repetition rate, and a beam diameter of ~2 mm at the interface. Less than 15% of the laser output power was coupled to the setup to not destroy the IMG. The fluctuation in the signal due to reducing the laser power limited the sensitivity of the system to monitor minor changes which may arise from pre-adsorption of sub-monolayers at temperatures higher than the dew point or freezing point.

25 Compared to the setup described in (Abdelmonem et al., 2015), a single fundamental beam incident on the interface was used and the SM (S-polarized SHG / 45°-polarized incident) polarization combination was measured. The polarization direction of the incident beam was controlled by a half-wave plate followed by a cube polarizer. The generated signal was collected using a photomultiplier tube (PMT) placed downstream of an optical system including the appropriate filters and a polarization analyzer. The incident angle from air of the fundamental beam was adjusted to 15° with respect to surface  
30 normal of the sapphire prism. The corresponding incident angle on the mica-air or -water interface was ~ 51.6°, which is higher than the critical angles of TIR for mica-air (~ 34.1°) and mica-water (~50.2°) interfaces. This guaranteed a TIR condition regardless of any changes in the Fresnel factors caused by the change of refractive indices with changing temperature. The advantage of using SM polarization combination is its dependence on only one non-vanishing nonlinear susceptibility tensor element ( $\chi_{yyz}$ ), (Shen, 1989b;Zhuang et al., 1999), at any working angle which makes it a direct probe  
35 of the degree of order of the molecules at the interface.

### 3 Results and discussion

The relative humidity (RH) of the purged gas was set to specific values in different runs to allow for different freezing modes on the surface of mica. Figure 1a shows the change in normalized Fresnel factor-corrected (see SI for details) SHG intensities under SM polarization combination for deposition freezing (DF) at -38 °C (black solid line and circles), -21 °C  
40 (red solid line and empty squares), and at -12.5 °C (green solid line and empty triangles) labeled by DF1, DF2, and DF3, respectively. In DF1, the cell was filled with N<sub>2</sub> gas and the sample was cooled down to a temperature, -38 °C, far below the



dew point at RH = 5 % (-21 °C). At -38 °C, the cell was purged with humid air of RH ~ 5 %. An ice-film formed immediately on the surface, reflected by a drop in the SHG signal compared to that of air-mica interface. In DF2 and DF3, the cell was purged continuously with humid air of RH = 5 and 11 %, respectively, and then cooled down until freezing and growth of ice were observed on the surface. Deposition freezing and the formation of an ice-film started at -21 and -12.5 °C for RH = 5 % (DF2) and 11 % (DF3), respectively. The results show a drop in the SHG signal with respect to the signal of the mica-air interface upon freezing for the three cases DF1, DF2, and DF3. However, the relative signal drop for DF1 differs from those of DF2 and DF3. DF2 and DF3 were observed at temperatures equal to the dew points at the preset RHs, indicating two-step nucleation, first condensation, and then freezing. The coincidence of the SHG signals of the thin ice-film formed in DF2 and DF3 indicates identical structuring of water on the surface in two-step deposition freezing regardless of the onset temperature. This means that at temperatures above -38 °C, growth of ice on mica apparently is a two-step process: Water first condenses and then freezes. This confirms on the molecular level the two-stage nucleation hypothesis which suggests that a nucleus forms as a liquid cluster and then freezes (Layton and Jr., 1963; Lupi et al., 2014). Further pumping of the gas mixture to the measuring cell allows for the growth of the ice-film by diffusion. The resulting ice-bulk shows a further drop in the signal for DF2 and DF3. This drop was not observed for DF1, thus indicating a major difference in the spectroscopic behavior of ice between one-step and two-step deposition freezing. To ensure that the lack of change in the SHG signal after the growth of an ice-film to ice-bulk in one-stage nucleation, DF1 figure 1a, is not an artefact, DF1 and DF2 were compared using a different system (sapphire-water interface, Fig. 1b). Figure 1b shows the change in SHG intensity at the surface of sapphire for DF at -38 (black solid line and circles) and at -23 °C (red solid line and empty squares) labeled by DF1 and DF2, respectively. As in the case of mica, the drop in SHG intensity after the formation of an ice-film was followed by another drop upon further pumping of humid air of RH = 5 % in the two-step freezing process (DF2), but not in one-step (DF1) freezing.

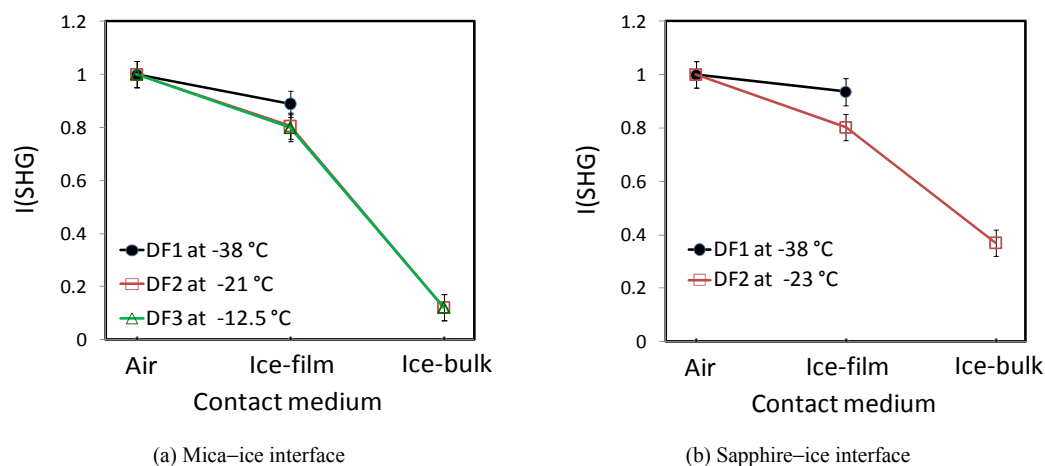


**Figure 1:** SHG intensity measured at the surfaces of mica (a) and sapphire (b) in contact with air, ice-film, and ice-bulk, respectively, collected in SM polarization combination during the three different cooling cycles, DF1: Sample cooled down first to -38 °C under dry N<sub>2</sub> gas, followed by pumping water vapor of RH = 5 % to the measuring cell. DF2: Sample cooled down under flow of water vapor of RH = 5 %. DF3: Sample cooled down under flow of water vapor of RH = 10 %. The signal is Fresnel-corrected and normalized to the air value. All connection lines between points are just for guiding the eyes.

Figure 2 shows three different freezing experiments at different RHs. The gas RH was adjusted to allow liquid condensation (LC) during cooling at temperatures higher than those of deposition freezing. Constant pumping of humid air at RH = 20, 30, and 40 % and cooling down resulted in the formation of stable liquid films at -3.5, 3, and 7 °C, respectively. At all RH values, the SHG signal drops down upon the formation of a liquid-film by LC. The relative drop of the signal with respect to



the air signal is similar to that observed in the DF experiments, Figure 1a. Comparing Figures 1a and 2, the SHG signals are in the same range regardless of the film phase (liquid or ice). By further pumping of humid air after LC, liquid–bulk forms at the surface with a signal that is lower than that of the liquid–film. This is mostly due to the contributions from the few secondary layers of the interfacial water. Further cooling of the sample in contact with liquid–bulk causes water to freeze by immersion freezing (IF). The observed IF temperatures for IF1, IF2, and IF3 are similar and center around  $-11\text{ °C} \pm 1\text{ °C}$  which is within the range of IF temperatures observed for freezing of bulk water in contact with the surface of mica in former studies (Abdelmonem et al., 2015; Anim-Danso et al., 2016). IF produced a transient ice phase with SHG intensity higher than that of the interfacial water of the bulk liquid. The lifetime of the transient phase is around one minute, Figure 3. The values of the SHG intensities plotted in Figure 2 for transient ice–bulk are the peak values found on the transient curves shown in Figure 3 after Fresnel factor corrections and normalization to the mica–air signal. The transient phase may have had peak values higher than those obtained from Figure 3, but they were not detected due to the fast signal decay right after nucleation and the limited time resolution of signal detection of about 2.5 sec. A transient phase lasting for several minutes was reported very recently by Lovering et al. using SFG at a water–silica interface (Lovering et al., 2017). They suggested a transient existence of stacking-disordered (non-centrosymmetric) ice during the freezing process at water–mineral interfaces. Anim-Danso et al. also observed such transient ice lasting for a few tens of seconds in SFG experiments at a high-pH (9.8) solution–sapphire interface. They suggested that charge transfer and the stitching bilayer are perturbed at high pH, which leads to a decrease in SFG intensity. The present work shows that the transient ice occurs at neutral pH on mica surface and has a significant nonresonant component which is observable with the simple SHG technique. Apparently, the lifetime of the transient phase depends on the substrate and probably on the liquid–bulk size and might play a big role in the ice nucleation ability of the surface. However, this requires a comparative study involving different substrates, which will be subject of future work.

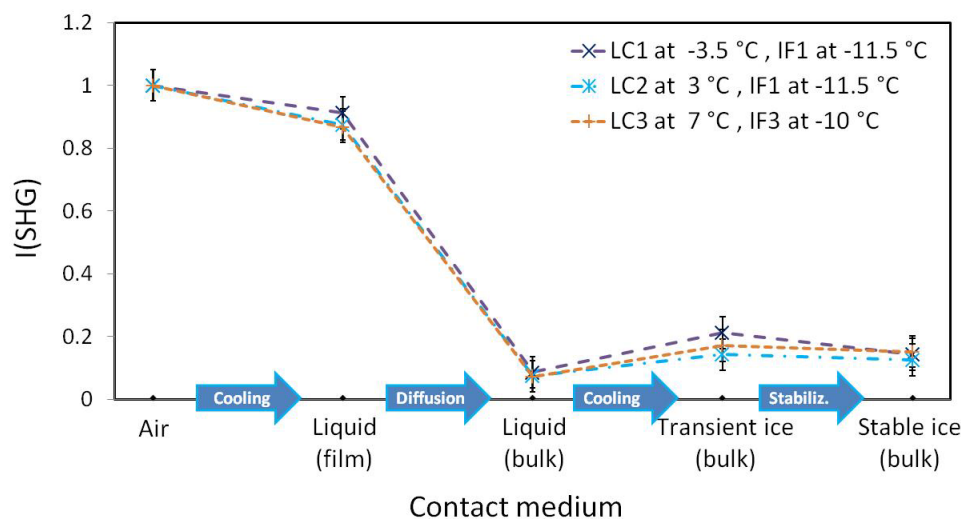
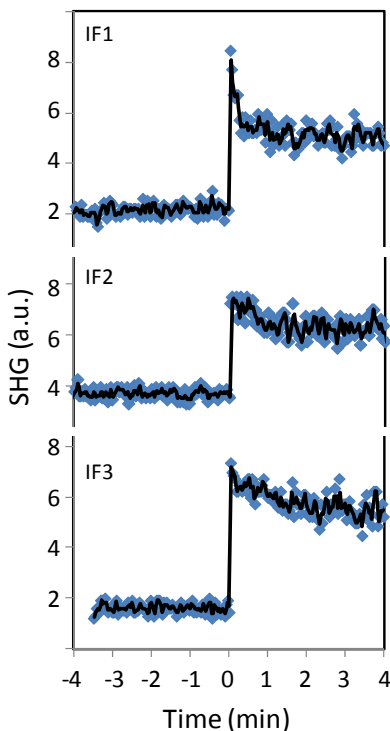


Figure 2: SHG intensity measured at the surface of mica in contact with air, liquid–film, liquid–bulk, transient ice–bulk, and stable ice–bulk, respectively, collected in SM polarization combination during three different cooling cycles, LC1 IF1: Sample cooled down under flow of water vapor of RH = 20 %. LC2 IF2: Sample cooled down under flow of water vapor of RH = 30 %. LC3 IF3: Sample cooled down under flow of water vapor of RH = 40 % (see text for details). The signal is Fresnel-corrected and normalized to the air value. All connection lines between points are just for guiding the eyes.



**Figure 3: Typical variation in the SHG intensity around the immersion freezing points for IF1, IF2, and IF3 during the cooling experiments**

Finally, I would like to comment on the drop, rather than increase, of the signal upon adsorption of water (or ice) on the surface (of either mica or sapphire). Since SHG response reflects the overall arrangements of the polar entities at the interface between two isotropic media (Fordyce et al., 2001; Goh et al., 1988; Luca et al., 1995), signal intensity is expected to increase when a single (or few non-centrosymmetric) layer(s) of water or ice is(are) formed at the surface. It is clear from Figures 1 and 2, however, that SHG intensity decreases upon deposition freezing, condensation, and growth of liquid layers by diffusion. This can be explained by phase interference between two signals originating from two different interfacial groups of opposite dipole moments: surface-OH points out of the surface and water-OH points to the surface. A cleaved mica surface exhibits a hexagonal arrangement of Si (partly Al) and O atoms which hydrate immediately in contact with air. The mica-air signal mainly originates from the surface hydroxyl groups (dangling-OH) which are naturally pointing out from the surface. Since mica surface is inherently negatively charged, the interfacial water-OH groups will point to the surface and thus have a phase opposite to that of the surface-OH groups, as was reported by Shen and co-workers (Zhang et al., 2008) on negatively charged surfaces. This well explains the ostensible decrease in the overall signal upon deposition and condensation. When the surface of mica is covered with bulk water, it becomes totally deprotonated (no free-OH) (Odelius et al., 1997). Under this condition the SHG signal comes exclusively from the interfacial water molecules between the surface and liquid-bulk. This defines a new reference of the signal generated at the new interface (liquid-solid rather than gas-solid). The increase of the signal afterwards indicates more structuring of either the interfacial water before freezing, like shown in (Abdelmonem et al., 2015) or interfacial ice after freezing like shown here.



## Conclusion

In summary, I used a simple SHG setup to discriminate and describe three different freezing paths on the surface of mica. The results decide on, and confirm on the molecular level, the previous speculations about the existence of two-stage deposition ice nucleation at temperatures above  $-38\text{ }^{\circ}\text{C}$ . One-step and two-step deposition freezing of a thin film of ice show water structure similar to that of a thin film of liquid water. When a liquid–bulk freezes at the surface by immersion freezing, there is a transient non-centrosymmetric ice phase of high non-resonant SHG signal. The lifetime of the transient phase is suggested to be substrate–dependent and expected to affect ice nucleation efficiency. The presented results open up new horizons for the role of aerosol surfaces in promoting and stabilizing heterogeneous ice nucleation. They provide novel molecular–level insight into different ice nucleation regimes using a simple spectroscopic technique. Investigating the structuring of water molecules upon freezing next to solid surfaces is crucial to many scientific areas, such as atmospheric physics and chemistry, hydrology, and environmental and industrial applications.

## Acknowledgements

The work is funded by the German Research Foundation (DFG, AB 604/1-1). The SHG setup was funded by the competence area “Earth and Environment” of KIT (start-up budget 2012). The author is grateful to Prof. Dr. T. Leisner, Dr. J. Lützenkirchen, Dr. C. Linke and Mrs. M. Schröder from the KIT for their support.

## References

- Abdelmonem, A., Lützenkirchen, J., and Leisner, T.: Probing ice-nucleation processes on the molecular level using second harmonic generation spectroscopy, *Atmos. Meas. Tech.*, 8, 3519-3526, doi: 10.5194/amt-8-3519-2015, 2015.
- Abdelmonem, A., Backus, E. H. G., Hoffmann, N., Sánchez, M. A., Cyran, J. D., Kiselev, A., and Bonn, M.: Surface charge-induced orientation of interfacial water suppresses heterogeneous ice nucleation on  $\alpha$ -alumina (0001), *Atmos. Chem. Phys. Discuss.*, 2017, 1-13, doi: 10.5194/acp-2017-224, 2017.
- Anim-Danso, E., Zhang, Y., and Dhinojwala, A.: Surface Charge Affects the Structure of Interfacial Ice, *J. Phys. Chem. C*, 120, 3741-3748, doi: 10.1021/acs.jpcc.5b08371, 2016.
- Balmer, T. E., Christenson, H. K., Spencer, N. D., and Heuberger, M.: The Effect of Surface Ions on Water Adsorption to Mica, *Langmuir*, 24, 1566-1569, doi: 10.1021/la702391m, 2008.
- Beaglehole, D., Radlinska, E. Z., Ninham, B. W., and Christenson, H. K.: Inadequacy of Lifshitz theory for thin liquid films, *Phys. Rev. Lett.*, 66, 2084-2087, 1991.
- Campbell, J. M., Meldrum, F. C., and Christenson, H. K.: Characterization of Preferred Crystal Nucleation Sites on Mica Surfaces, *Cryst. Growth Des.*, 13, 1915-1925, doi: 10.1021/cg301715n, 2013.
- DeMott, P. J., Möhler, O., Stetzer, O., Vali, G., Levin, Z., Petters, M. D., Murakami, M., Leisner, T., Bundke, U., Klein, H., Kanji, Z. A., Cotton, R., Jones, H., Benz, S., Brinkmann, M., Rzesanke, D., Saathoff, H., Nicolet, M., Saito, A., Nillius, B., Bingemer, H., Abbatt, J., Ardon, K., Ganor, E., Georgakopoulos, D. G., and Saunders, C.: Resurgence in Ice Nuclei Measurement Research, *Bull. Am. Meteorol. Soc.*, 92, 1623-1635, doi: 10.1175/2011bams3119.1, 2011.
- Eastwood, M. L., Cremel, S., Gehrke, C., Girard, E., and Bertram, A. K.: Ice nucleation on mineral dust particles: Onset conditions, nucleation rates and contact angles, *J. Geophys. Res.: Atmospheres*, 113, 203-201 - 203-209, doi: 10.1029/2008jd010639, 2008.
- Fordyce, A. J., Bullock, W. J., Timson, A. J., Haslam, S., Spencer-Smith, R. D., Alexander, A., and Frey, J. G.: The temperature dependence of surface second-harmonic generation from the air-water interface, *Mol. Phys.*, 99, 677-687, doi: 10.1080/00268970010030022, 2001.
- Goh, M. C., Hicks, J. M., Kemnitz, K., Pinto, G. R., Heinz, T. F., Eisenthal, K. B., and Bhattacharyya, K.: Absolute orientation of water molecules at the neat water surface, *J. Phys. Chem.*, 92, 5074-5075, doi: 10.1021/j100329a003, 1988.
- Hoose, C. and Mohler, O.: Heterogeneous ice nucleation on atmospheric aerosols: a review of results from laboratory experiments, *Atmos. Chem. Phys.*, 12, 9817-9854, doi: 10.5194/acp-12-9817-2012, 2012.
- Hu, J., Xiao, X.-D., Ogletree, D. F., and Salmeron, M.: Imaging the Condensation and Evaporation of Molecularly Thin Films of Water with Nanometer Resolution, *Science*, 268, 267-269, doi: 10.1126/science.268.5208.267, 1995.
- Jang, J. H., Lydiatt, F., Lindsay, R., and Baldelli, S.: Quantitative Orientation Analysis by Sum Frequency Generation in the Presence of Near-Resonant Background Signal: Acetonitrile on Rutile TiO<sub>2</sub> (110), *J. Phys. Chem. A*, 117, 6288-6302, doi: 10.1021/jp401019p, 2013.
- Layton, R. G. and Jr., F. S. H.: Nucleation of Ice on Mica, *J. Atmos. Sci.*, 20, 142-148, doi: 10.1175/1520-0469(1963)020<0142:noiom>2.0.co;2, 1963.
- Lovering, K. A., Bertram, A. K., and Chou, K. C.: Transient Phase of Ice Observed by Sum Frequency Generation at the Water/Mineral Interface During Freezing, *J. Phys. Chem. Lett.*, 8, 871-875, doi: 10.1021/acs.jpcclett.6b02920, 2017.
- Luca, A. A. T., Hebert, P., Brevet, P. F., and Girault, H. H.: Surface second-harmonic generation at air/solvent and solvent/solvent interfaces, *J. Chem. Soc. Faraday Trans.*, 91, 1763-1768, doi: 10.1039/f9959101763, 1995.



- Lupi, L., Kastelowitz, N., and Molinero, V.: Vapor deposition of water on graphitic surfaces: Formation of amorphous ice, bilayer ice, ice I, and liquid water, *J. Chem. Phys.*, 141, 18C508, doi: 10.1063/1.4895543, 2014.
- Mason, B. J. and Maybank, J.: Ice-nucleating properties of some natural mineral dusts, *Q. J. R. Meteorol. Soc.*, 84, 235-241, doi: 10.1002/qj.49708436104, 1958.
- 5 Odelius, M., Bernasconi, M., and Parrinello, M.: Two Dimensional Ice Adsorbed on Mica Surface, *Phys. Rev. Lett.*, 78, 2855-2858, doi: 10.1103/PhysRevLett.78.2855, 1997.
- Poppa, H. and Elliot, A. G.: The surface composition of Mica substrates, *Surf. Sci.*, 24, 149-163, doi: 10.1016/0039-6028(71)90225-1, 1971.
- Pruppacher, H. R. and Klett, J. D.: *Microphysics of clouds and precipitation*, 2 ed., Atmospheric and oceanographic sciences library, 18, Kluwer Academic Publishers, Dordrecht ; Boston, 954 pp., 1997.
- 10 Rao, Y., Tao, Y.-s., and Wang, H.-f.: Quantitative analysis of orientational order in the molecular monolayer by surface second harmonic generation, *J. Chem. Phys.*, 119, 5226-5236, doi: 10.1063/1.1597195, 2003.
- Schaefer, V. J.: The Formation of Ice Crystals in the Laboratory and the Atmosphere, *Chem. Rev.*, 44, 291-320, doi: 10.1021/cr60138a004, 1949.
- 15 Shen, Y. R.: Surface properties probed by second-harmonic and sum-frequency generation, *Nature*, 337, 519-525, doi: 10.1038/337519a0, 1989a.
- Shen, Y. R.: Optical Second Harmonic Generation at Interfaces, *Annu. Rev. Phys. Chem.*, 40, 327-350, doi: 10.1146/annurev.pc.40.100189.001551, 1989b.
- Slater, B., Michaelides, A., Salzmann, C. G., and Lohmann, U.: A Blue-Sky Approach to Understanding Cloud Formation, *Bull. Am. Meteorol. Soc.*, 97, 1797-1802, doi: 10.1175/bams-d-15-00131.1, 2016.
- 20 Zhang, L., Tian, C., Waychunas, G. A., and Shen, Y. R.: Structures and Charging of  $\alpha$ -Alumina (0001)/Water Interfaces Studied by Sum-Frequency Vibrational Spectroscopy, *J. Am. Chem. Soc.*, 130, 7686-7694, doi: 10.1021/ja8011116, 2008.
- Zhuang, X., Miranda, P. B., Kim, D., and Shen, Y. R.: Mapping molecular orientation and conformation at interfaces by surface nonlinear optics, *Phys. Rev. B*, 59, 12632-12640, doi: 10.1103/PhysRevB.59.12632, 1999.

25